Engineering and Technology Journal e-ISSN: 2456-3358
Volume 10 Issue 04 April-2025, Page No.- 4406-4412
DOI: 10.47191/etj/v10i04.05, I.F. – 8.482

Comparative Analysis of Monohull and Catamaran Passenger Vessels: Performance in Shallow Waters

Benjamin Golfin Tentua[1], Samy Junus Litiloly[1], Richard Benny Luhulima[2]
[1]Mechanical Engineering Department, Faculty of Engineering, Universitas Pattimura, Ambon, Indonesia
[2]Naval Architecture Department, Faculty of Engineering, Universitas Pattimura, Ambon, Indonesia

ABSTRACT: This study investigated modifying a 500 GT monohull passenger vessel into a catamaran while maintaining displacement with the aim of enhancing resistance. Computational Fluid Dynamics (CFD) analysis, following the International Towing Tank Conference (ITTC) protocols, was employed to simulate fluid flow around vessel geometries. Simulations were conducted at 8 knots in shallow water with a depth of 3 m, resulting in a depth-to-draft ratio (h/t) of 1.5. The results showed that the monohull experienced a 102.56 kN resistance, which is 35% higher than that of the catamaran's 35.73 kN. The resistance of the monohull was influenced by the increased fluid flow velocity around the bow and stern, leading to a greater hull-water interaction. Pressure distribution analysis highlighted elevated pressure on the monohull bow due to high-velocity fluid interactions, while the catamaran configuration effectively managed the load distribution. Power calculations, assuming 50% efficiency, determined that the monohull required a 566 hp engine, whereas the catamaran required 197 hp. These findings emphasize the impact of vessel design on performance and efficiency, providing insights into engine selection and operational efficiency in maritime engineering.

KEYWORDS: Passenger Ship, Monohull, Catamaran, Resistance, Power

I. INTRODUCTION

The development of monohull passenger ships into catamarans for shallow-water operations stems from the evolving demands for efficiency, stability, and adaptability in maritime transport. Historically, monohulls dominated due to their simplicity and traditional design, rooted in early seafaring cultures [1]. However, their single-hull structure poses challenges in shallow waters, where deeper drafts limit access to coastal or inland routes. Monohulls also generate higher resistance at higher speeds, increasing fuel consumption and operational costs [2]. Passenger vessels with the potential to operate in shallow waters are those with a tonnage of 500 GT. An example of such a passenger ship is the KMP Takabonerate, as illustrated in Figure 1.

Figure 1 KMP. Takabonerate [3]

Catamarans, with their twin-hull configuration, address these limitations by offering a shallower draft, enabling operation in waters unsuitable for monohulls [4] . Their wider beams enhance transverse stability, reduce roll motions, and improve passenger comfort [5]. Studies highlight that catamarans experience lower resistance compared to monohulls at high speeds, particularly in shallow waters, where hydrodynamic interactions like wave formation and trim adjustments significantly impact performance [6].

Design advancements, such as bulbous bows and computational optimization of hull forms, have further refined catamarans for shallow-water efficiency, minimizing drag and improving seakeeping [7]. While monohulls retain advantages in rough seas due to their self-righting keels [8], catamarans excel in payload capacity and operational flexibility, making them ideal for modern passenger ferry services in ecologically sensitive or restricted-depth areas. This shift reflects a broader industry trend toward specialized, environmentally conscious designs tailored to niche operational environments [9, 10].

Catamarans are frequently chosen for operation in shallow waters because of their hydrodynamic properties, although they encounter unique resistance issues in these environments. The design of catamarans, characterized by their catamaran structure, results in reduced water resistance compared to that of traditional monohulls. This is primarily attributed to their streamlined hulls, which effectively minimize drag, coupled with their lighter overall weight that enhances their efficiency across varying water depths [11].

However, shallow water dynamics present specific challenges for catamarans. Under such conditions, the pressure distribution around the vessel changes significantly; the pressure at the midship decreases, while the pressure at the bow and stern increases. This alteration can lead to the formation of a "critical wave" that is perpendicular to the catamaran's direction of travel, causing the bow to rise and increasing the overall resistance. Consequently, the total resistance experienced by the vessel escalates due to the limitations on wave formation and the disruption of flow dynamics inherent in shallow water [12].

To address these challenges, design adaptations are essential to optimize catamaran performance in shallow environments. Research efforts are directed towards refining aspects such as resistance, trim, and sinkage at elevated speeds [13]. Innovations in hull shapes and the incorporation of transom sterns have been explored to reduce wave interference and enhance stability under shallow conditions. Both numerical simulations and experimental methods, including towing tank tests, were employed to confirm the hydrodynamic efficiency of these vessels, even with increased resistance. Ultimately, while shallow water conditions may elevate resistance, catamarans retain significant advantages over monohulls, particularly in terms of transverse stability and payload capacity, making them well-suited for applications like high-speed, zero-emission transport in shallow regions.[14].

This study aimed to evaluate the modification of a monohull passenger vessel into a catamaran while maintaining the same displacement, a transformation that could potentially enhance the vessel's performance and stability in various marine environments. The analysis is conducted using Computational Fluid Dynamics (CFD), a sophisticated numerical method that allows for the simulation of fluid flow around complex geometries, following the rigorous protocols established by the International Towing Tank Conference (ITTC) [15, 16]. This process begins with the meticulous creation of the model geometry, which involves accurately representing the physical characteristics of both the monohull and newly designed catamaran. Subsequently, appropriate boundary conditions were set to reflect the operational environment, thereby ensuring that the simulations yielded realistic and applicable results. A critical aspect of CFD analysis is the verification of grid independence, which guarantees that the results are not significantly affected by the resolution of the computational mesh. Both models were subjected to simulations at the operational speed of the vessel, specifically 8 knots, in a shallow water scenario characterized by a river depth of 3 m. This results in a depth-to-draft ratio (h/t) of 1.5, which is particularly relevant for assessing the resistance performance of catamaran hulls in shallow water environments.

II. METHOD

A. *Governing Equation*

When performing wake-field modeling, the selection of the correct turbulence model is crucial. This research considered the Shear Stress Transport (SST) turbulence model, which was developed by Menter [17, 18]. The SST model has been widely used and validated by many researchers, who have found it to produce satisfactory outcomes [19][20]. The RANS solver, a part of ANSYS CFX, was used to address the fluid flow field. Equations (1), (2), and (3) represent the continuity, RANS, and SST turbulence equations, respectively:

Continuity equation:

$$\frac{\partial \rho}{\partial t} + \frac{\partial}{\partial x_j}\left(\rho U_j\right) = 0 \tag{1}$$

In the continuity equation, ρ is the fluid density, *t* is time, *and* U_j is the flow velocity vector field.

RANS equation:

$$\rho \bar{f}_i + \frac{\partial}{\partial x_j}\left[-\bar{p}\delta_{ij} + \mu\left(\frac{\partial \bar{u}_i}{\partial x_j} + \frac{\partial \bar{u}_j}{\partial x_i}\right) - \overline{\rho u_i' u_j'}\right] - \rho \bar{u}_j \frac{\partial \bar{u}_i}{\partial x_j} = 0 \tag{2}$$

The left side of the RANS equation (2) represents the change in the mean momentum of the fluid element with unsteadiness in mean flow. This change is balanced by the mean body force ($\bar{f}$), the mean pressure field ($\bar{p}$), the viscous stress, $\mu\left(\frac{\partial \bar{u}_i}{\partial x_j} + \frac{\partial \bar{u}_j}{\partial x_i}\right)$, and apparent stress ($\rho u_i' u_j'$) to the fluctuating velocity field.

Menter’s SST equation

$$\frac{\gamma}{v_t}P - \beta\rho\omega^2 + \frac{\partial}{\partial x_j}\left[\left(\mu + \sigma_\omega \mu_t\right)\frac{\partial \omega}{\partial x_j}\right] + 2\left(1 - F_1\right)2\rho_{\omega 2}\frac{1}{\omega}\frac{\partial k}{\partial x_j}\frac{\partial \omega}{\partial x_j} - \left(\frac{\partial(\rho\omega)}{\partial t} + \frac{\partial\left(\rho u_j \omega\right)}{\partial x_j}\right) = 0 \tag{3}$$

The SST model developed by Menter integrates the benefits of the k–ω model to present an enhanced formulation applicable to a range of scenarios. To accomplish this, a blending function F1 was introduced, which assumes a value of one in regions adjacent to the solid surface and zero in the flow domain further from the wall. This approach facilitates the activation of the k–ω model near the walls and the k–ε model for the remaining flow, thereby leveraging the advantageous near-wall performance of the k–ω model to assess the sensitivity of the freestream.

B. *Numerical model*

Geometry Model

Computational fluid dynamics (CFD) analysis was conducted on a monohull passenger vessel with a gross tonnage of 500 GT, along with its modification into a catamaran while maintaining the same displacement. This is illustrated in Figure 2, and the principal dimensions are listed in Table 1.

(a) Monohull

(b) Catamaran

Figure 2 Ship Model Geometry

Table 1 Particular Dimension of Passenger Ship

Dimension	Unit	Monohull	Catamaran
Length Over All (LOA)	m	40	50
Length of Water Line (LWL)	m	42.2	48.5
Height (H)	m	4	5
Breadth (B)	m	12	24
Hull Spacing (S)	m	-	18
Draft (T)	m	2	
Wetted Surface Area (WSA)	m^2	515.51	662.7
Displacement (Δ)	Ton	755	754
Water Density (ρ)	Kg/m^3	998	

Boundary Condition

The optimal computational domain for modeling the intake velocity is generally established at a distance of 2 L in the front, oriented perpendicular to the front surface. Additionally, a pressure outlet was situated 5 L towards the rear and aligned perpendicularly. To mitigate the influence of the transverse pressure, adjustments were made in both the transverse and vertical orientations. To avert the occurrence of backflow, Ford and Winroth [21] introduced a pressure exit outflow as the downstream boundary condition, as illustrated in Figure 3(a).

The configuration of the boundary conditions and the dimensions of the domain are shown in Figure 3(b). An opening condition was applied to the upper wall, whereas the sidewalls were treated with symmetry conditions. The hull body was designated as a fixed boundary, and a no-slip condition was imposed on the model to ensure accurate flow representation. The inlet flow velocity was 8 knots, with the outlet pressure being dependent on the water level. Furthermore, the initial location of the free surface was articulated through the specification of volume fraction functions for both water and air at the entry and exit points of the system, which were essential for determining the quantities of water and air present in the system.

Meshing and Grid Independence Study

Effective modelling using a hybrid mesh is a sophisticated technique that addresses the accuracy issues encountered near the walls of a computational model, as illustrated in Figure 4. In fluid dynamics and other engineering simulations, the behavior of flow near boundaries is crucial because it often dictates the overall performance and efficiency of the system being analyzed. Traditional uniform mesh approaches cannot capture the intricate details of flow behavior in these regions, leading to potential inaccuracies in the results. Engineers can achieve a more refined representation of the geometry and flow characteristics by employing a hybrid mesh that integrates various mesh types, such as structured, unstructured, and adaptive meshes. This tailored approach allows for a denser mesh in areas of high gradient, such as near walls, while maintaining a coarser mesh in regions where the flow is more uniform, thus optimizing computational resources without sacrificing accuracy [22]

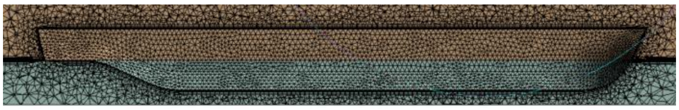

(a) Side view

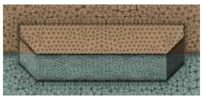

(i) monohull

(ii) catamaran

(b) Mid Ship

Figure 4 Hybrid mesh for ship model

It is likely that the use of a fine mesh in ANSYS CFX consistently produces reliable results. However, the complexity and number of components involved lead to an increase in the computational time and resources required for analysis. It is essential to consider mesh size during the computational phase. The assessment of the mesh convergence for both ship passenger models is illustrated in Figure 3. For the sails, a total mesh count of approximately 1.72 million was reached for monohull and about 1.81 million for catamaran model, signifying that optimal mesh convergence has been attained. This observation is further corroborated by the findings of Anderson [23], which indicate that the variation in the total drag coefficient is less than 2%.

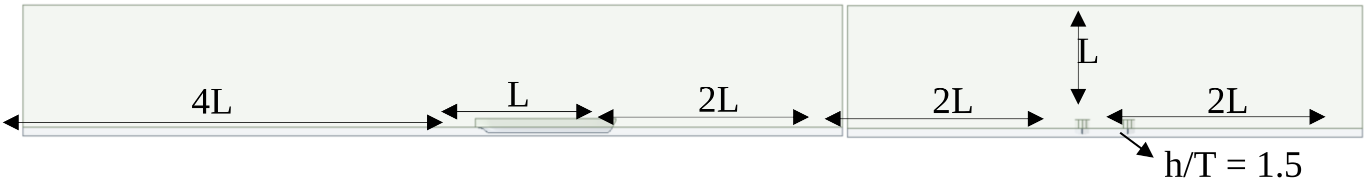

(a) Model Distance to Boundary

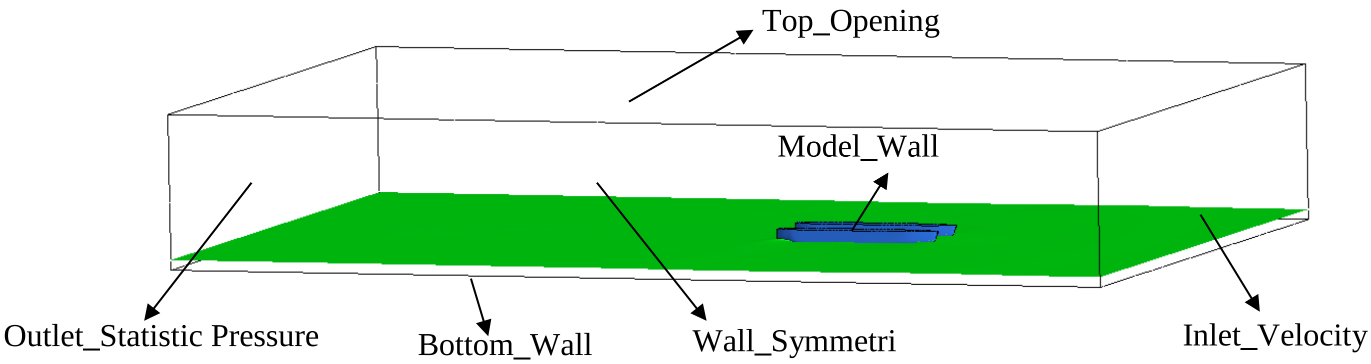

(b) Boundary Condition

Figure 3 Setup Model Passenger Ship

III.RESULT AND DISCUSSION

A. Resistance Analysis

The simulation results reveal that the resistance encountered by the monohull passenger vessel is recorded at 102.56 kN, in contrast to the catamaran model, which shows a resistance of 35.73 kN. This comparison highlights that the resistance of the monohull is 35% higher than that of the catamaran, a relationship visually represented in Figure 4. Such a significant difference in resistance underscores the performance characteristics of each vessel type, suggesting that the monohull design may face greater hydrodynamic challenges than the more efficient catamaran configuration. The implications of these results are critical for understanding the operational efficiency and potential fuel consumption of each vessel and guiding future design considerations in maritime engineering.

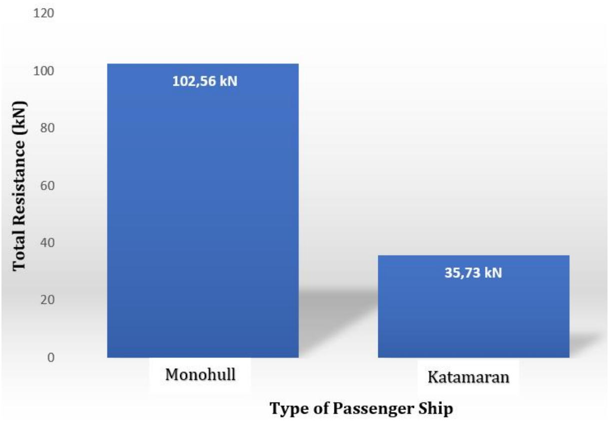

Figure 4 Resistance Result of Numerical simulation

The resistance experienced by the monohull passenger vessels was notably influenced by a significant increase in the fluid flow velocity around the bow and stern, as shown in Figure 5(a). In shallow waters, this heightened fluid flow leads to greater interaction between the hull of the passenger ship and the surrounding water. In contrast, the hull of a catamaran does not exhibit any significant changes in the flow velocity beneath its structure, indicating a different hydrodynamic behavior compared to the monohull designs.

Moreover, the design of catamarans, with their catamaran configuration, allows for a more stable and efficient interaction with water, minimizing the adverse effects of increased flow velocity, as shown in Figure 5(b). This characteristic can be particularly advantageous in various maritime applications, where performance and efficiency are paramount. Therefore, the choice between monohull and catamaran designs should be carefully considered based on the intended operational environment and performance requirements.

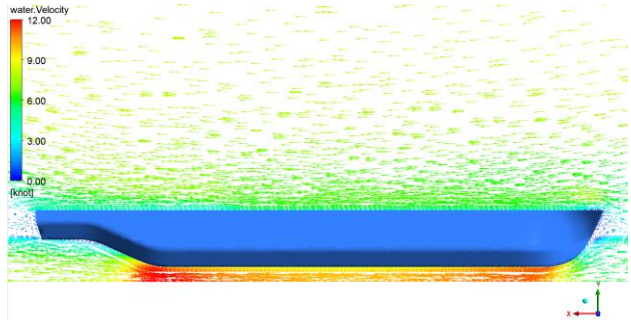

(a) Monohull

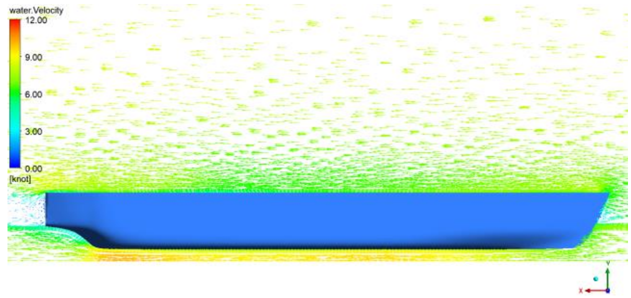

(b) Catamaran

Figure 5 Water flow velocity at Shallow water

The dynamics of fluid flow around these two types of vessels highlight the distinct challenges faced by monohulls, particularly in shallow environments, where increased flow can exacerbate resistance. This interaction not only affects the performance of the vessel, but also has implications for fuel efficiency and overall operational effectiveness. Understanding these differences is crucial for naval architects and engineers when designing vessels for specific water conditions.

The results of this simulation are complemented by a visualization of the monohull bow, depicted in red, which illustrates the increase in pressure resulting from interactions with high-velocity fluids, as shown in Fig.6 (a). This elevated pressure effect leads to significant resistance experienced by the monohull vessel.

Furthermore, the graphical representation effectively highlights the critical areas in which fluid dynamics play a crucial role in influencing vessel performance. The interaction between the hull and the surrounding fluid at high speeds not only contributes to the pressure increase but also underscores the challenges faced in optimizing the design for improved hydrodynamic efficiency.

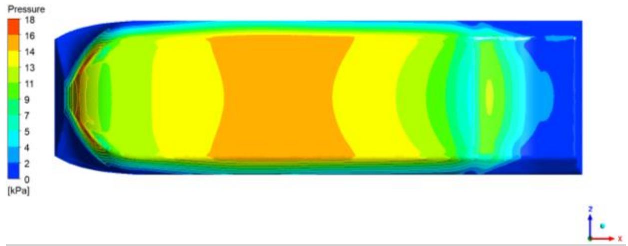

(a) monohull

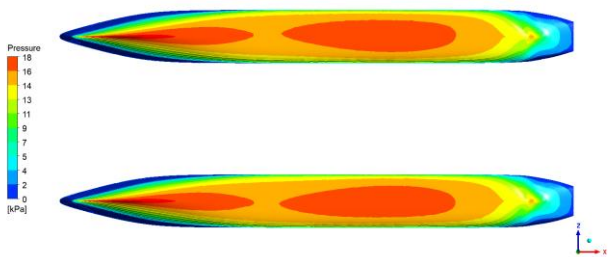

(b) Catamaran

Figure 6 Pressure Distribution at both model

In passenger catamarans, there was also an increase in the stress observed in the bow and central hull sections of the vessel. However, the relatively small surface area of the catamaran's hull mitigates the overall impact, as the pressure is distributed across both hulls of the catamaran, as show Figure

This stress distribution is crucial in maintaining the structural integrity of the vessel, allowing it to withstand various operational conditions without significant risk of failure. The design of the catamaran, with its configuration, plays a vital role in effectively managing these forces, ensuring that the load is shared evenly, and reducing the likelihood of localized stress concentrations that could compromise the safety and performance of the ship.

B. Power Need

The calculation of power is a fundamental concept in physics and engineering and is often defined as the rate at which work is done or energy is needed to overcome resistance at a given speed. To quantify this relationship, the formula for power can be expressed as

$$EHP = R_T \times v \tag{4}$$

where EHP represents the effective horsepower, R_T denotes the Total Resistance, and v is the service vlocity. This formula highlights the direct correlation between the amount of work performed and the duration over which that work occurs.

The estimation of machinery requirements is based on power calculations using the following formula: The effective horsepower (EHP) represents the pure power generated by the propeller. Assuming a power efficiency of 50%, the primary engine requirement for a monohull passenger vessel is calculated to be 566 hp, whereas for a catamaran passenger vessel, the requirement is determined to be 197 hp, As Shown Figure 7.

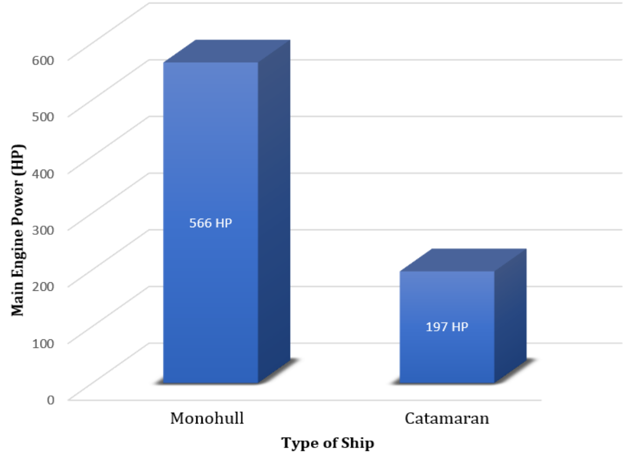

Figure 7 Power Need for Both Model of Passenger ship

This analysis highlights the significant differences in engine power requirements between different types of passenger vessels, emphasizing the impact of vessel design on performance and efficiency. The calculations underscore the importance of accurately assessing power requirements to ensure optimal engine selection and operational efficiency in maritime engineering.

CONCLUSIONS

An analysis utilizing Computational Fluid Dynamics (CFD) was performed to evaluate the performance of monohull and catamaran passenger vessels operating under shallow water conditions. The simulations were executed at a speed of 8 knots, specifically in a scenario characterized by a water depth-to-draft ratio of 1.5. The findings revealed that the monohull vessel encountered a resistance that was 35% greater than that of the catamaran, with the monohull registering a resistance of 102.56 kN compared to the catamaran's 35.73 kN. This disparity in resistance can be attributed to the increased fluid flow velocity around the bow and stern of the monohull, which results in heightened drag forces.

The unique catamaran configuration contributed to a more stable and efficient interaction with water, thereby reducing resistance. Further analysis of the pressure distribution indicated that the bow of the monohull experienced elevated pressure levels owing to high-velocity fluid interactions occurring in that region. In terms of power requirements, calculations indicated that the monohull required a significantly more powerful engine, rated at 566 hp, while the catamaran was adequately powered by a 197 HP engine. This stark contrast in power requirements underscores the efficiency advantages offered by catamaran design for shallow water navigation.

ACKNOWLEDGMENT

We extend our heartfelt gratitude to the Design and Simulation Laboratory Team at Universitas Pattimura for their invaluable support in successfully completing the study.

REFERENCES

1. "Monohull vs Catamaran: A Deep Dive into Design and Performance." Retrieved March 27, 2025, from https://info.sailingvirgins.com/blog/monohull-vs-catamaran-a-deep-dive-into-design-and-performance
2. Seif, M., and Amani, E. "Performance comparison between planing monohull and catamran at high Froude numbers." Iranian Journal of Science and Technology Transactions of Mechanical Engineering, Vol. 28, No. 4, (2004), 435–441. https://doi.org/10.22099/ijstm.2013.969
3. "Resmi Dilaunching, Kapal KMP Takabonerate Akan Tiba Di Selayar Bulan Desember - Selayarnews.com." Retrieved March 28, 2025, from https://selayarnews.com/05/11/2020/resmi-dilaunching-kapal-kmp-takabonerate-akan-tiba-di-selayar-bulan-desember/
4. "Building Catamarans - RARCC - Raja Ampat Research & Conservation Centre." Retrieved March 27, 2025, from https://stichting-rarcc.org/projects/educationawareness-projects/building-catamarans/
5. Ulgen, K., and Dhanak, M. R. "Hydrodynamic Performance of a Catamaran in Shallow Waters." Journal of Marine Science and Engineering, Vol. 10, No. 9, (2022), 1169. https://doi.org/10.3390/jmse10091169
6. Everest, J. T. Some Research on the Hydrodynamics of Catamarans and Multi-hulled Vessels in Calm Water. North East Coast Institution of Engineers and Shipbuilders. Retrieved from https://books.google.co.id/books?id=Lz1JOAAACAAJ
7. Mittendorf, M., and Papanikolaou, A. D. "Hydrodynamic hull form optimization of fast catamarans using surrogate models." Ship Technology Research, Vol. 68, No. 1, (2021), 14–26. https://doi.org/10.1080/09377255.2020.1802165
8. "Catamaran vs. Monohull: We Changed, Should You? | The Catamaran Gurus." Retrieved March 27, 2025, from https://catamaranguru.com/catamaran-vs-monohull-we-changed-should-you/
9. Kusuma, C., Ariana, I. M., and Ali, B. "Redesign KCR 60m Bow with Axe Bow Type To Reduce Ship Resistance." IOP Conference Series: Earth and Environmental Science, Vol. 557, No. 1, (2020), 012033.https://doi.org/10.1088/1755-1315/557/1/012033
10. Gittens, J. E., Smith, T. J., Suleiman, R., and Akid, R. "Current and emerging environmentally-friendly systems for fouling control in the marine environment." Biotechnology Advances, Vol. 31, No. 8, (2013), 1738–1753. https://doi.org/10.1016/J.BIOTECHADV.2013.09.002
11. Martić, I., Degiuli, N., Borčić, K., and Grlj, C. G. "Numerical Assessment of the Resistance of a Solar Catamaran in Shallow Water." Journal of Marine Science and Engineering, Vol. 11, No. 9, (2023), 1706. https://doi.org/10.3390/jmse11091706
12. Duman, S., Boulougouris, E., Aung, M. Z., Xu, X., and Nazemian, A. "Numerical Evaluation of the Wave-Making Resistance of a Zero-Emission Fast Passenger Ferry Operating in Shallow Water by Using the Double-Body Approach." Journal of Marine Science and Engineering, Vol. 11, No. 1, (2023), 187. https://doi.org/10.3390/jmse11010187
13. Ali, A., Maimun, A., Ahmed, Y. M., and Rahimuddin. "Resistance analysis of a semi-SWATH design concept in shallow water." Journal of Marine Science and Application, Vol. 16, No. 2, (2017), 182–189. https://doi.org/10.1007/s11804-017-1406-x
14. "Catamarans: Advantages and Downsides of a double-hulled." Retrieved March 27, 2025, from https://partyboatcharter.com/catamarans-advantages/
15. ITTC. ITTC-Recommended Procedures and Guidelines: Practical Guidelines for Ship CFD Applications. 26th ITTC Specialist Committee on CFD in Marine Hydrodynamics.
16. ITTC. "ITTC – Recommended Procedures and Guidelines - Practical guidelines for ship CFD applications. 7.5-03-02-03 (Revision 01)." In 27th International Conference Towing Tank (pp. 31 August–5 September. Denmark).
17. Menter, F. R. "Two-equation eddy-viscosity turbulence models for engineering applications." AIAA Journal, Vol. 32, No. 8, (1994), 1598–1605. https://doi.org/10.2514/3.12149
18. Menter, F. R. "Zonal two equation κ-ω turbulence models for aerodynamic flows." In AIAA 23rd Fluid Dynamics, Plasmadynamics, and Lasers Conference, 1993 (pp. 1–21).
19. ANSYS. "ANSYS® Academic Research." ANSYS CFX-Solver Modeling Guide, (2013).
20. Bayraktar, E., Mierka, O., and Turek, S. "Benchmark computations of 3D laminar flow around a cylinder with CFX, OpenFOAM and FeatFlow." International

Journal of Computational Science and Engineering, Vol. 7, No. 3, (2012), 253–266. https://doi.org/10.1504/IJCSE.2012.048245

21. Ford, C. L., and Winroth, P. M. “On the scaling and topology of confined bluff-body flows.” Journal of Fluid Mechanics, No. 876, (2019), 1018–1040. https://doi.org/10.1017/jfm.2019.583
22. Tu, J., Yeoh, G.-H., and Liu, C. “Chapter 4-CFD Mesh Generation: A Practical Guideline.” In Computational Fluid Dynamics (Third Edit., pp. 125–154). UK: Elsevier. https://doi.org/10.1016/B978-0-08-101127-0.00004-0
23. Anderson, J. D. Computational Fluid Dynamics: The Basics with Applications. New York, USA. pp. 526-532: McGraw-Hill. Retrieved from https://books.google.co.id/books?id=phG_QgAACAAJ